

AD-A040 921

DAVID W TAYLOR NAVAL SHIP RESEARCH AND DEVELOPMENT CE--ETC F/G 1/3  
HOVER EVALUATION OF THE CIRCULATION CONTROL HIGH SPEED ROTOR.(U)  
JUN 77 K R READER

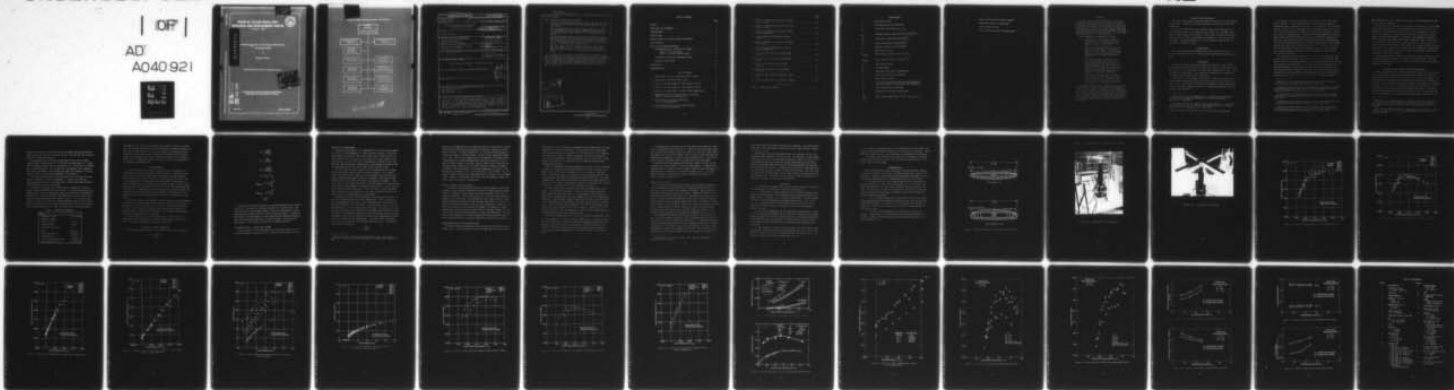
UNCLASSIFIED

AERO-1239

DTNSRDC-77-0034

NL

| OF |  
AD  
A040 921



END

DATE

FILMED

7-77

Report 77-0034

HOVER EVALUATION OF THE CIRCULATION CONTROL HIGH SPEED ROTOR

12

J

# DAVID W. TAYLOR NAVAL SHIP RESEARCH AND DEVELOPMENT CENTER



Bethesda, Md. 20884

ADA 040921

## HOVER EVALUATION OF THE CIRCULATION CONTROL HIGH SPEED ROTOR

by

Kenneth R. Reader

APPROVED FOR PUBLIC RELEASE: DISTRIBUTION UNLIMITED

DDC  
RECEIVED  
JUN 24 1977  
LIBRARY

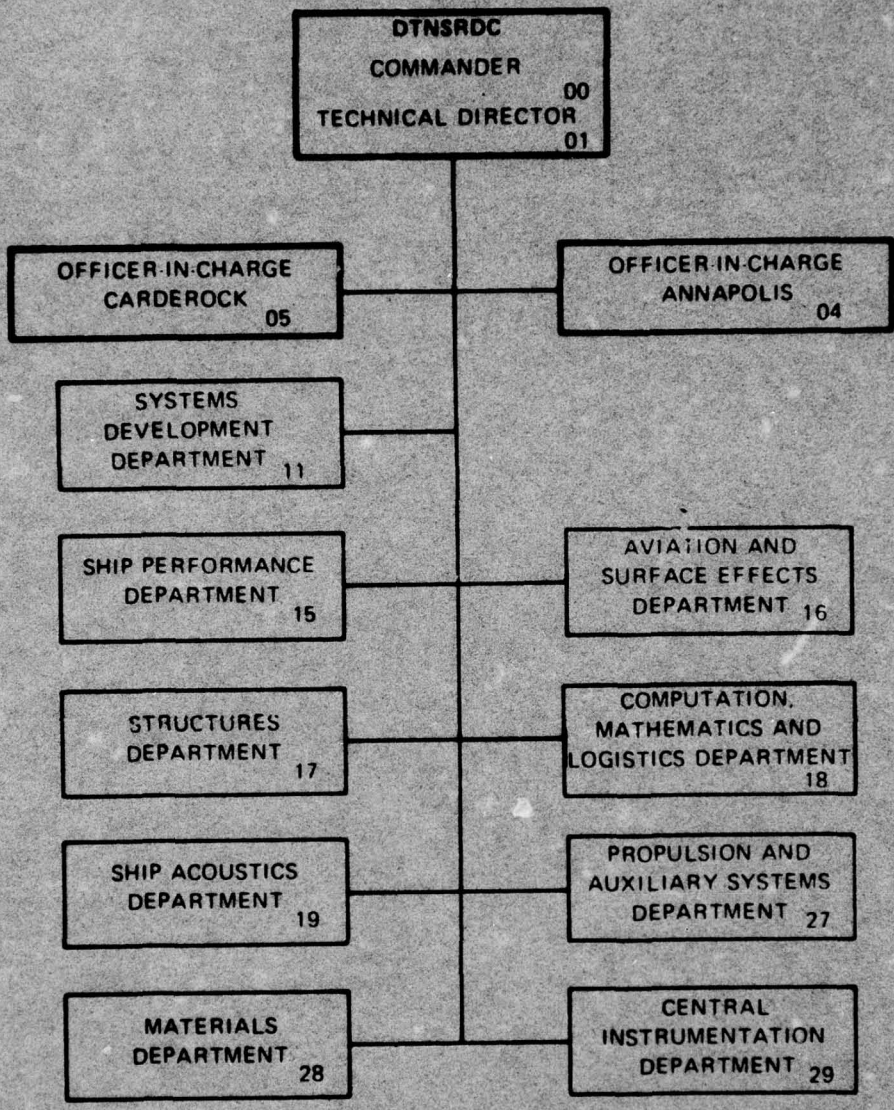
AD No. \_\_\_\_\_  
DDC FILE COPY

AVIATION AND SURFACE EFFECTS DEPARTMENT  
RESEARCH AND DEVELOPMENT REPORT

June 1977

Report 77-0034

MAJOR DTNSRDC ORGANIZATIONAL COMPONENTS



BEST AVAILABLE COPY

UNCLASSIFIED

SECURITY CLASSIFICATION OF THIS PAGE (When Data Entered)

REPORT DOCUMENTATION PAGE		READ INSTRUCTIONS BEFORE COMPLETING FORM	
1. REPORT NUMBER DTNSRDC 77-0034	2. GOVT ACCESSION NO.	3. RECIPIENT'S CATALOG NUMBER	
4. TITLE (and Subtitle) HOVER EVALUATION OF THE CIRCULATION CONTROL HIGH SPEED ROTOR	5. TYPE OF REPORT & PERIOD COVERED		
7. AUTHOR(s) Kenneth R. Reader	6. PERFORMING ORG. REPORT NUMBER Aero Report -1239		
9. PERFORMING ORGANIZATION NAME AND ADDRESS David W. Taylor Naval Ship Research and Development Center Bethesda, Maryland 20084	10. PROGRAM ELEMENT, PROJECT, TASK AREA & WORK UNIT NUMBERS Project F41.421.210 Work Unit 1-1690-111		
11. CONTROLLING OFFICE NAME AND ADDRESS Naval Air Systems Command - AIR-320D Washington, D.C. 20361	12. REPORT DATE June 1977		
14. MONITORING AGENCY NAME & ADDRESS (if different from Controlling Office) F41421 WF41421210	13. NUMBER OF PAGES 40 (123386)		
16. DISTRIBUTION STATEMENT (of this Report)  APPROVED FOR PUBLIC RELEASE: DISTRIBUTION UNLIMITED	15. SECURITY CLASS. (of this report) UNCLASSIFIED		
17. DISTRIBUTION STATEMENT (of the abstract entered in Block 20, if different from Report)	15a. DECLASSIFICATION/DOWNGRADING SCHEDULE		
18. SUPPLEMENTARY NOTES			
19. KEY WORDS (Continue on reverse side if necessary and identify by block number) Circulation Control Rotors Hover Evaluation High Speed Rotor - Hover			
20. ABSTRACT (Continue on reverse side if necessary and identify by block number) As part of the on-going Circulation Control Rotor Technology Program at the David W. Taylor Naval Ship Research and Development Center (DTNSRDC), a high-speed rotor model, designated the RB-CCR (reverse blowing circulation control rotor), was evaluated in the hover mode. The experiments utilized an existing DTNSRDC model hover stand and the model was tested as a two- and four-bladed rotor with several rotor configurations.  (Continued on reverse side)			

DDC  
APPROVED  
JUN 24 1977  
UNCLASSIFIED

DD FORM 1473 1 JAN 73

EDITION OF 1 NOV 65 IS OBSOLETE  
S/N 0102-LF-014-6601

UNCLASSIFIED

SECURITY CLASSIFICATION OF THIS PAGE (When Data Entered)

387695 ✓

(Block 20 continued)

Major findings are summarized as follows:

1. The best rotor performance in hover at a particular  $C_T/\sigma$  is established from tradeoffs between tip Mach number and blade collective pitch angle.
2. With the leading edge slot covered, augmentation of rotor thrust was independent of tip Mach number. Thrust augmentation was reduced by approximately 18 percent when the leading edge slot was exposed.
3. The increased power required in hover due to the exposed leading edge slot indicates that some means of closing off the leading edge slot (when not in use) should be incorporated into a full-scale rotor. (One suggested means might be a flexible slot lip with slot opening a function of blade duct pressure.)
4. There was a small reduction in figure of merit for the trailing edge slot closed off (slot cutout) for 30-percent radius and as much as a 6-percent reduction in performance for a 50-percent slot cutout.

In general the hover tests demonstrated that a good figure of merit can be obtained over a large range of collective pitch angles. A comparison of configurations at various collective angles showed a steady improvement in performance with increasing collective pitch angle (up to  $\theta_c = 6$  deg). Indeed, the RB-CCR model demonstrated that the high-speed rotor can hover with a zero mechanical collective pitch angle at a figure of merit of about 0.50.

*(cont. p. 1)*

*A*

*theta sub c*

APPROVED BY	WRITE SECTION	<input checked="" type="checkbox"/>
DATE	BUFF SECTION	<input type="checkbox"/>
UNCLASSIFIED		<input type="checkbox"/>
JUSTIFICATION		
SY		
DISTRIBUTION/AVAILABILITY CODES		
Dist.	AVAIL. and/or SPECIAL	
<i>A</i>		

## TABLE OF CONTENTS

	Page
ABSTRACT . . . . .	1
ADMINISTRATIVE INFORMATION . . . . .	2
ACKNOWLEDGMENT . . . . .	2
INTRODUCTION . . . . .	2
REVERSE BLOWING CIRCULATION CONTROL ROTOR MODEL . . . . .	4
TEST PROCEDURE . . . . .	6
EVALUATION OF HOVER PERFORMANCE . . . . .	6
TWO-BLADED RESULTS — LEADING EDGE COVERED . . . . .	7
Effects of Tip Mach Number . . . . .	8
Effects of Blade Collective Angle . . . . .	9
COMPARISON OF TWO- AND FOUR-BLADED ROTORS . . . . .	9
EFFECTS OF SLOT CUTOUT . . . . .	11
CONCLUSIONS . . . . .	12
RECOMMENDATIONS . . . . .	13

## LIST OF FIGURES

1 - RB-CCR Model Rotor Tip and Root Airfoil Profiles . . . . .	14
2 - RB-CCR Model on DTNSRDC Hover Stand . . . . .	15
3 - Effect of Tip Mach Number on Shaft Figure of Merit . . . . .	17
4 - Effect of Tip Mach Number on Total Figure of Merit . . . . .	18
5 - Effect of Tip Mach Number on Rotor Thrust Augmentation . . . . .	19
6 - Expanded Scales to Illustrate Effect of Tip Mach Number on Rotor Thrust Augmentation . . . . .	20
7 - Rotor Thrust versus Blade Pressure at Various Tip Mach Numbers . . . . .	21
8 - Rotor Weight Flow Rate versus Blade Pressure at Various Tip Mach Numbers . . . . .	22

	Page
9 - Effect of Collective Pitch Angle on Shaft Figure of Merit . . . . .	23
10 - Effect of Collective Pitch Angle on Total Figure of Merit . . . . .	24
11 - Effect of Collective Pitch Angle on Rotor Thrust Augmentation . . . . .	25
12 - Leading Edge Slot and Solidity Effects in Hover . . . . .	26
13 - Hover Performance of Two- and Four-Bladed RB-CCR Rotor . . . . .	26
14 - Effect of Rotor Configuration on Rotor Thrust Augmentation . . . . .	27
15 - Effect of Slot Cutout with Leading Edge Covered . . . . .	28
16 - Effect of Slot Cutout with Leading Edge Exposed . . . . .	29
17 - Effect of Root Cutout on Root Blade Pressure . . . . .	30
18 - Effect of Root Cutout on Rotor Weight Flow Rate . . . . .	30
19 - Effect of Root Cutout on Compressor Power Ratio . . . . .	31
20 - Effect of Root Cutout on Total Rotor Power . . . . .	31
-----	
Table 1 - Model Rotor Geometry . . . . .	5

## NOMENCLATURE

b	Blade span in feet
$C_L$	Two-dimensional lift coefficient
$C_P$	Total power coefficient; $C_{P_S} + C_{P_C}$
$C_{P_C}$	Compressor power coefficient; $\dot{m} V_j^2 / (2\rho\pi R^2 V_T^3)$
$C_{P_S}$	Shaft power coefficient; $Q\Omega / (\rho\pi R^2 V_T^3)$
$C_T$	Thrust coefficient; thrust / $(\rho\pi R^2 V_T^2)$
$C_\mu$	Blowing coefficient; $\dot{m} V_j / (\rho\pi R^2 V_T^2)$
c	Blade chord in feet
$FM_{\text{Shaft}}$	Shaft figure of merit; $0.707 C_T^{1.5} / C_{P_S}$
$FM_{\text{Total}}$	Total figure of merit; $0.707 C_T^{1.5} / C_P$
h	Slot height in feet
$M_T$	Tip Mach number
$\dot{m}$	Total mass flow rate in slugs/second
Q	Rotor shaft torque in foot-pound
R	Rotor radius in feet
$V_j$	Jet velocity calculated from the peak blade root pressure expanded to free-stream static pressures
$V_T$	Rotor tip speed in feet/second
x	Dimensionless distance along radius
$\frac{\Delta C_L}{\Delta C_{\mu_R}}$	Rotor thrust augmentation (slope of $C_T$ versus $C_{\mu_R}$ )

$\theta_c$  Blade collective pitch angle in degree  
 $\rho$  Atmosphere density in slugs/feet<sup>3</sup>  
 $\sigma$  Rotor solidity,  $4c/\pi b$   
 $\Omega$  Rotor rotational speed in radians/second

## ABSTRACT

As part of the on-going Circulation Control Rotor Technology Program at the David W. Taylor Naval Ship Research and Development Center (DTNSRDC), a high-speed rotor model designated the RB-CCR (reverse blowing circulation control rotor) was evaluated in the hover mode. The experiments utilized an existing DTNSRDC model hover stand and the model was tested as a two- and four-bladed rotor with several rotor configurations.

Major findings are summarized as follows:

1. The best rotor performance in hover at a particular  $C_T/\sigma$  is established from tradeoffs between tip Mach number and blade collective pitch angle.
2. With the leading edge slot covered, augmentation of rotor thrust was independent of tip Mach number. Thrust augmentation was reduced by approximately 18 percent when the leading edge slot was exposed.
3. The increased power required in hover due to the exposed leading edge slot indicates that some means of closing off the leading edge slot (when not in use) should be incorporated into a full-scale rotor. (One suggested means might be a flexible slot lip with slot opening a function of blade duct pressure.)
4. There was a small reduction in figure of merit for the trailing edge slot closed off (slot cutout) for 30-percent radius and as much as a 6-percent reduction in performance for a 50-percent slot cutout.

In general the hover tests demonstrated that a good figure of merit can be obtained over a large range of collective pitch angles. A comparison of configurations at various collective angles showed a steady improvement in performance with increasing collective pitch angle (up to  $\theta_c = 6$  deg). Indeed, the RB-CCR model demonstrated that the high-speed rotor can hover with a zero mechanical collective pitch angle at a figure of merit of about 0.50.

#### ADMINISTRATIVE INFORMATION

The work reported herein was sponsored by the Naval Air Systems Command (NAVAIR 320). Funding was provided under Project F41.421.210, Work Unit I-1619-111.

All data recorded during this experiment were either measured in or converted directly to U.S. customary units. Hence, U.S. customary units are the primary units in this report. Metric units are given either adjacent to the U.S. units in parentheses or opposite U.S. units in the case of graphs. Angular measurement is the only exception; degrees were not converted to radians on graphs.

#### ACKNOWLEDGMENT

The author gratefully acknowledges the significant contribution of Mr. Drew Linck who assisted in conducting the experiments and reducing the data.

#### INTRODUCTION

The application of circulation control (CC) airfoils to helicopters was predicated on their ability to increase the airfoil 2-dimensional lift coefficient ( $C_l$ ) at fixed angle of attack and to generate very high  $C_l$  without angle of attack stall. CC airfoils have demonstrated the capability to provide these characteristics by blowing.

The concept of a circulation control rotor (CCR) has been well established through industrial studies and extensive wind tunnel evaluations on model scale. The literature provides well-documented results and descriptions of the basic concept as applied to helicopters operating in the conventional speed regime.<sup>1-7</sup>

---

<sup>1</sup>Smith, M.C.G., "The Aerodynamics of a Circulation Controlled Rotor," 3rd CAL/AVLABS Symposium on Aerodynamics of Rotary Wing Aircraft, Buffalo, N.Y. (Jun 1969).

<sup>2</sup>Williams, R.M. and E.O. Rogers, "Design Considerations of Circulation Control Rotors," Paper 603, 28th National Annual Forum of the American Helicopter Society, Washington, D.C. (May 1972).

NOTE: References are continued at the bottom of the following page.

In principle, the concept involves a shaft-driven rotor and blades with CC airfoils. These airfoils employ a rounded trailing edge and tangentially eject a thin jet of air from a slot adjacent to this (Coanda) surface. Airfoil lift is proportional to the momentum flux of this jet of air. The CCR requires an air supply duct within each blade and a continuous supply of compressed air. A simple throttling mechanism in the rotor head provides control over both the cyclic and collective components of blown air, thus meeting cyclic and collective rotor control requirements. This process eliminates the need for blade mechanical cyclic pitch changes and may eliminate that for mechanical collective pitch also. Being free of numerous dynamic control system components, the rotor head therefore has a greatly simplified mechanism and also presents a cleaner profile from the drag standpoint.

The above concept has been extended at DTNSRDC to a high-speed, high-advance ratio rotor system. This rotor system is also shaft driven and employs CC airfoil sections modified by incorporating blowing slots on both the leading and trailing edges. A unique control system enables both azimuthal programming of the blowing to the leading edge slot and the controllability needed to maintain rotor trim. Such a rotor concept has potential both as a reduced-rpm, thrust-compounded helicopter with speeds approaching 400 knots and as a stoppable rotor aircraft with speeds

---

<sup>3</sup>Wilkerson, J.B., "Design and Performance Analysis of a Prototype Circulation Control Rotor," NSRDC ASED AL-290 (Mar 1973).

<sup>4</sup>Wilkerson, J.B. and D.W. Linck, "A Model Rotor Validation for the CCR Technology Demonstrator," Paper 902, 31st National Annual Forum of the American Helicopter Society, Washington, D.C. (May 1975).

<sup>5</sup>"Design Study of a Flight Worthy Circulation Control Rotor System," Kaman Aerospace Corporation Report R-1036-2, Contract N00019-73-C-0429 (Jul 1974).

<sup>6</sup>"Design Study of a Helicopter with a Circulation Control Rotor (CCR)," Lockheed Report LR26417, Contract N00019-73-C-0435 (May 1974).

<sup>7</sup>Reader, K.R. and Wilkerson, J.B., "Circulation Control Applied to a High Speed Helicopter Rotor," Paper 1003, 32nd National Annual Forum of the American Helicopter Society, Washington, D.C. (May 1976).

approaching Mach 1.0.<sup>8</sup> A complete discussion of the high-speed rotor concept is already available.<sup>7</sup>

The present report evaluates the performance of an 80-in. (2.03 m) high-speed rotor model in hover. This RB-CCR model was tested as both a two-bladed and a four-bladed rotor for various rotor configurations. The test variables included rotor thrust, blade collective pitch angle, tip Mach number, and rotor configuration. The major rotor parameters measured on the hover stand (total power, shaft power, compressor power, rotor thrust, rotor efficiency, mass flow rate, blade pressure, etc.) were plotted in coefficient form for constant tip Mach number and constant blade collective pitch angle. The various rotor configurations evaluated were leading edge slot exposed and covered, two and four blades, and clockwise and counter-clockwise rotation of the blades.

Because of the large volume of data obtained in these experiments, only the most significant findings and tradeoffs are reported here. The complete (unpublished) data set is on file in the Aviation and Surface Effects Department at DTNSRDC.

#### REVERSE BLOWING CIRCULATION CONTROL ROTOR MODEL

Analytical studies of the RB-CCR concept were used to establish a baseline rotor design in terms of operational thrust coefficient-to-solidity ratio, blade twist, and airfoil distributions of thickness and camber. The resulting RB-CCR configuration was designed and manufactured at DTNSRDC as an 80-in. (2.03 m) diameter four-bladed untwisted rotor model for evaluation in the 8- × 10-ft (2.44 × 3.05 m) North Subsonic Wind Tunnel and on the hover stand of the Aviation and Surface Effects Department.\* The airfoil sections were symmetrical about the midchord with both a leading edge slot and a trailing edge slot. Thickness distribution varied linearly from 20

---

<sup>8</sup>Williams, R.M., "Application of Circulation Control Rotor Technology to a Stopped Rotor Aircraft Design," presented at the First European Rotorcraft and Powered Lift Aircraft Forum, Southampton, England (22-24 Sep 1976).

\*This work was conducted under the sponsorship of the Naval Air Systems Command. The analytical study was performed, among others, by Mr. E.O. Rogers at DTNSRDC.

percent at the root to 15 percent at the tip; camber distribution varied from 5 percent at the root to zero at the tip. The root and tip CC airfoil profiles are shown in Figure 1.

Slot positions were a constant percentage of chord over the blade radius; namely (leading edge)  $x/c = 0.032$  and (trailing edge)  $x/c = 0.968$ . The slot-height-to-chord ratio was constant at  $h/c = 0.002$  for both leading and trailing edge slots. Air for each slot was supplied from a separate duct within the blade so that blowing from either the leading or trailing edge slot could be controlled independently (see Figure 1).

The blades were machined from solid aluminum alloy in upper and lower halves by numerically controlled machines. Internal ducts and slot-regulating posts were cut at the same time to ensure equal mass and stiffness distributions between the blades.

The physical characteristics of the model are summarized in Table 1. Figure 2 shows the RB-CCR in the wind tunnel. It should be noted that the model solidity ratio is considerably larger than what would be designed or required for a full-scale RB-CCR. The scaled chord for the correct solidity would have resulted in a model chord of 2.8 in. (7.11 cm) and a slot height of 0.0056 in. (0.0142 cm). The requirement of two slots per blade (and two air supply ducts per blade) made this small chord very impractical from a manufacturing point of view. Therefore the chord was arbitrarily

TABLE 1 - MODEL ROTOR GEOMETRY

Blade	
Diameter, ft (m)	6.67 (2.08)
Number of Blades	4
Chord, in. (cm)	5 (12.7)
Solidity Ratio	0.1592
Geometric Twist, deg	0
Airfoil	
Thickness Ratio $t/C$	0.20/0.15
Camber Ratio $\delta/C$	0.05/0.0
Trailing Edge Radius $R_{TE}/C$	0.052/0.022
Slot Height Ratio $h/c$	0.002/0.002

increased to 5 in. (12.7 cm), allowing a slot height of 0.010 in. (0.0254 cm). It was also realized that this increase would increase loads and provide more accurate data at the reduced tip speeds corresponding to model operation at high advance ratio. Basically this approach gave the model blades a lower aspect ratio than the full-scale design (8.0 as opposed to 10-12) and so the model data cannot be taken as directly representative of a full-scale, high-speed rotor.

#### TEST PROCEDURE

The RB-CCR model was evaluated in hover as both a two-bladed and a four-bladed rotor with corresponding solidity ratios of 0.0796 and 0.1592. The test variables in hover were thrust (controlled by blade pressure), blade collective pitch angle (0-10 deg), tip Mach number (0.26-0.55) and rotor configuration. At each blade collective angle, various values of tip Mach number were set and the model was tested through a range of blade pressures (blowing coefficient  $C_{\mu}$ ) from 0 to 10 psig. The two-bladed rotor configuration was evaluated with the leading edge slot covered and with the leading edge slot uncovered but with no blowing. The maximum thrust obtained was limited by the hydraulic power unit used to provide rotor shaft power.

All data were taken on the DTNSRDC hover test stand. Forces and moments were measured on a four-component Lebow balance system and recorded automatically on a Beckman data acquisition system. The data were reduced to coefficient form by an existing data reduction program and plotted on a Calcomp plotter. Tares due to the hydraulic and air supply lines were removed from the measured forces and moments.

Data were taken over a tip speed range of 300 to 650 fps (91.4 to 198.1 m/s), which corresponds to a Reynolds number range of  $0.8 \times 10^6$  to  $1.72 \times 10^6$  based on model blade chord and tip velocity.

#### EVALUATION OF HOVER PERFORMANCE

The following equations were used to evaluate rotor hover performance:

$$C_T = \frac{T}{\rho \pi R^2 V_T^2}$$

$$C_{\mu} = \frac{\dot{m} v_j}{\rho \pi R^2 V_T^2}$$

$$C_{P_s} = \frac{Q\Omega}{\rho \pi R^2 V_T^3}$$

$$C_{P_c} = \frac{\dot{m} v_j^2}{2\rho \pi R^2 V_T^3}$$

$$C_P = C_{P_s} + C_{P_c}$$

$$FM_{\text{Shaft}} = 0.707 \frac{C_T^{1.5}}{C_{P_s}}$$

$$FM_{\text{Total}} = 0.707 \frac{C_T^{1.5}}{C_P}$$

$$\sigma = \frac{4c}{\pi b}$$

Although the RB-CCR was designed for optimum performance at an advance ratio of 0.7, it proved to have good efficiency in the hover mode. The improved airfoil trailing edge design of this rotor demonstrated reduced compressibility effects relative to those reported earlier.<sup>4</sup> At high tip Mach number, the augmentation of rotor thrust was not adversely affected, and the profile power showed only a slight increase. A more detailed presentation of the results is given in the following sections.

#### TWO-BLADED RESULTS - LEADING EDGE COVERED

Typical results for the two-bladed rotor with leading edge slots covered are presented in Figures 3-8 for a blade collective angle of 6 deg.

### Effects of Tip Mach Number

CC airfoils have shown a lift compressibility effect with Mach number. The effect of this phenomenon on rotor performance is seen in the hover data presented in Figures 3 and 4 where shaft figure of merit and total rotor figure of merit as shown for six different tip Mach numbers (0.26, 0.39, 0.43, 0.47, 0.51, 0.55) with corresponding tip speeds of 300, 450, 500, 550, 600, and 650 fps, respectively; corresponding tip speeds in metric units were 90.9, 136.4, 151.5, 166.7, 181.9, and 197.0 mps.

The shaft figure of merit reflects the increased power due to blade profile and induced drag as blade tip speed increases. At a constant thrust coefficient, shaft figure of merit decreases with increasing tip speed, indicating that profile power is increasing. The trends of shaft figure of merit with thrust coefficient are presented in Figure 3. The total figure of merit shows the effect of tip Mach number and blade loading on the total power required by the model rotor (Figure 4). Except for the lowest tip Mach number tested ( $M_T = 0.26$ ), the figure of merit decreased with increasing tip Mach number; at  $\Theta_c = 6$  deg, its maximum value was between  $0.10 < C_T/\sigma < 0.12$  depending on tip Mach number.

A measure of how well the RB-CCR airfoils sections generate thrust can be seen by examining the rotor thrust augmentation. This is analogous to the lift augmentation data have for the two-dimensional investigation of CC airfoils<sup>9</sup> wherein lift coefficient  $C_L$  was plotted as a function of blowing coefficient  $C_{\mu}$  for a constant angle of attack. The slope of the resultant curve ( $\Delta C_L/\Delta C_{\mu}$ ) is an indication of the augmentation capability of the CC airfoil. This same performance evaluation can be made for the CC rotor; see Figures 5 and 6 for an indication of rotor thrust augmentation and the effect of tip speed on that augmentation. The rotor thrust coefficient  $C_T/\sigma$  is plotted versus the rotor blowing coefficient  $C_{\mu_R}/\sigma$ . The blowing coefficient is defined as

$$C_{\mu_R} = \frac{\dot{m} V_j}{\rho \pi R^2 V_T^2}$$

---

<sup>9</sup>Stone, M.B. and R.J. Englar, "Circulation Control - A Bibliography of NSRDC Research and Selected Outside References, " NSRDC Report 4108 (Jan 1974).

where  $\dot{m}$  is the measured rotor air mass flow and  $V_j$  is the slot jet velocity calculated by isentropically expanding the blade root pressure to atmospheric pressure. The data presented are for a blade collective angle of 6 deg and a range of tip Mach numbers. Except for the lowest Mach number ( $M_T = 0.26$ ), rotor thrust augmentation was independent of tip Mach number. A comparison of the RB-CCR augmentation ratio with previous CC rotors like the higher harmonic circulation control (HHCC) clearly indicates the increased thrust capability of the RB-CCR design for similar increments of blowing. More specifically, the thrust augmentation ( $\Delta C_T / \Delta C_\mu$ ) of the RB-CCR was 24 compared to 18.3 for the CCR and 9.4 for the HHCC. For convenience Figure 6 presents the augmentation data of Figure 5 on an expanded scale. Figures 7 and 8 present the rotor thrust and measured weight flow versus blade root pressure, respectively.

#### Effects of Blade Collective Angle

In addition to determining the effect of tip Mach number on rotor performance, it was desired to determine the effect of blade collective angle as well. Examples of these results are shown in Figures 9 and 10 for a constant tip speed of 450 fps (136.4 m/s),  $M_T = 0.39$ , and blade collective angles of 4, 6, and 8 deg. The comparison of shaft figure of merit versus thrust coefficient-to-solidity ratio indicated that there is a collective angle above which shaft power increases rather drastically (Figure 9). The total rotor figure of merit includes the benefits of blowing; a tradeoff between blade collective angle and the amount of blowing is needed in order to establish the best rotor performance at each  $C_T/\sigma$  (Figure 10). The rotor shows a small degradation in thrust augmentation with increased blade collective angle as blowing is initially applied ( $C_\mu/\sigma < 0.003$ ); see Figure 11.

#### COMPARISON OF TWO- AND FOUR-BLADED ROTORS

The RB-CCR model was operated in hover as both a two-bladed and a four-bladed rotor. It was anticipated that the leading edge slot could cause a

power penalty, so the two-bladed configuration was evaluated with the leading edge slot both open and covered. (The condition with leading edge slots covered enables the performance of the present rotor to be compared with previous CC rotors.) Radial covering was effected by taping over the slot, thus providing a smooth aerodynamic shape to local flow in that region of the airfoil. An increase in total power was noted with the leading edge slot open.

Figure 12 shows that the power increase at the lower thrust coefficients was due to an increase in shaft power and that a further increase at the higher thrust coefficients was mainly due to an increase in compressor power. The power increase attributable to the open leading edge slot gave a corresponding reduction in hover figure of merit relative to the covered configuration. That reduction indicates that when the leading edge slot is not in use, some means of concealing it should be incorporated into a full-scale rotor. A flexible slot lip is one possible solution.

The four-bladed rotor was tested only with the leading edge slot exposed. Its performance was equal to that of the two-bladed rotor with leading edge exposed; see Figure 13. This agreement in hover figure of merit with the leading edge slots open suggests that the four-bladed rotor would have a much improved figure of merit with the slots covered (similar to the performance of the two-bladed rotor with covered slots at the same  $C_T/\sigma$ ). Figure 13 also shows the tendency of the rotor to maintain a relatively flat hover efficiency curve over a broad  $C_T/\sigma$  range, even for the constant collective pitch setting shown. This is a basic characteristic of the RB-CCR model and of prior CCR model rotors.

Rotor thrust augmentation ratio ( $\Delta C_T / \Delta C_{\mu_R}$ ) provides an additional check on the performance of the two- and four-bladed rotors. A comparison of the two- and four-bladed configurations indicated approximately the same augmentation ratio (17.0 and 16.3, respectively) for both solidities; see Figure 14. When the leading edge slot of the blade was covered however, an increase in thrust augmentation of 18 percent (from 17.0 to 20.8) was noted.

The maximum thrust obtained for the four-bladed rotor does not represent an aerodynamic thrust limitation. Instead it is a shaft power limitation caused by the hydraulic power unit used to provide rotor shaft power. The highest  $C_T/\sigma$  for the four-bladed rotor occurred at about the same disk loading as the highest  $C_T/\sigma$  shown for the two-bladed rotor. The two end points therefore represent about the same shaft torque requirement.

The RB-CCR model has demonstrated that good figures of merit can be obtained over a large range of collective pitch angles. A comparison of configurations at various collective angles showed a steady improvement in performance with increasing collective pitch angle (up to  $\theta_c = 6$  deg). Indeed, with zero collective pitch angle, operation was possible at a figure of merit of about 0.50.

#### EFFECTS OF SLOT CUTOUT

In conventional helicopter blade design, the aerodynamic lifting surface is eliminated in the inboard 10- to 20-percent radius because of a compromise between weight and aerodynamic efficiency. This position of the blade is referred to as the root cutout. Cassarino<sup>10</sup> found a 5- to 7-percent loss in hovering efficiency for a 50-percent root cutout at  $C_T/\sigma = 0.09$ . CC rotors can have an additional cutout type of effect since the inboard airfoil can be configured without the slot. To evaluate the slot cutout effect on CC rotor models, the slot is closed over different lengths of the inboard radius to simulate several slot root cutout conditions. Wilkerson and Linck<sup>4</sup> showed that in forward flight the effect of a 30-percent cutout of radius on total power was negligible at  $C_T/\sigma = 0.10$ .

The two-bladed RB-CCR model was tested in hover for slot cutouts of 14-, 30-, and 50-percent radius for both the leading edge slots covered and exposed; see Figures 15 and 16, respectively. It should be noted that no forced blowing was permitted from the leading edge slot in the exposed configuration. The effect of slot cutouts became more important to rotor performance at higher blade loadings ( $C_T/\sigma > 0.08$ ). There was only a small reduction in hover figure of merit for a root cutout of 30 percent but

---

<sup>10</sup>Cassarino, S.J., "Effect of Root Cutout on Hover Performance," AFFDL-TR-70-70 (Jun 1970).

above that value, much larger reductions were measured. More specifically, there was as much as 6-percent reduction in rotor figure of merit (Figure 15) at  $C_T/\sigma = 0.12$ .

Rotor weight flow rate and maximum blade root pressure are the rotor parameters most affected by the slot cutout. The variation of these parameters with slot cutout are presented in Figures 17 and 18 for  $C_T/\sigma = 0.12$ . The trends for both the covered and exposed configuration are the same, namely, decreasing weight flow rate and increasing maximum blade pressure with increasing slot cutout. A comparison of the ratio of compressor power to total power indicates a slight increase with additional slot cutout and the shaft power to total power shows a slight decrease with additional slot cutout (Figure 19). The effect of slot cutout on total rotor power was a substantial increase in total power (Figure 20).

#### CONCLUSIONS

1. The model has demonstrated that good figures of merit in hover can be obtained over a large range of collective pitch angles.

2. A comparison of configurations at various collective angles indicated a steady improvement in performance with increasing collective pitch angle (up to  $\Theta_c = 6$  deg). For a collective blade angle of 6 deg the figure of merit for the RB-CCR model was a maximum between  $0.10 < C_T/\sigma < 0.12$ .

3. A tradeoff between tip Mach number and blade collective pitch angle must be made in order to establish the best rotor performance in hover at each  $C_T/\sigma$ .

4. The thrust augmentation of the RB-CCR model exceeded that of other CC rotors evaluated at DTNSRDC over the past years. Within the Mach number range evaluated, the rotor with leading edge slot covered demonstrated that thrust augmentation is independent of tip Mach number and that the effect of the exposed leading edge slot was to decrease thrust augmentation by 18 percent.

5. The reduction in figure of merit in hover due to the exposed leading edge slot indicates that when the leading edge slot is not in use, some means of closing it off must be incorporated into a full-scale rotor. One possibility might be a flexible leading edge slot lip.

6. With no trailing edge slot on the inboard of the rotor blade, the figure of merit was slightly reduced for a slot cutout of 30 percent. Above that value, however, much larger reductions in performance were measured.

7. A basic characteristic of the RB-CCR is its tendency to maintain a high level of hover efficiency over a broad  $C_T/\sigma$  range even with a constant collective blade angle.

#### RECOMMENDATIONS

Since results from the hover evaluation of the RB-CCR model showed no limitations in hover, the concept is considered technically viable in the hover mode. However, several additional experimental investigations would broaden the understanding of the high-speed rotor in the hover mode:

1. Increased collective pitch angle range should be determined for the four-bladed rotor. The test data obtained for the four-bladed rotor model were limited by the shaft power available from the hydraulic power unit. Additional tests should be performed with the hydraulic power unit fixed to obtain rotor performance at higher collective pitch angles for the four-bladed RB-CCR model.

2. A set of rounded blown tips for mounting on the existing blades have been manufactured and should be evaluated on both the two- and four-bladed RB-CCR models. The square tips of the present RB-CCR blades are simple but not effective in reducing the strong tip vortex generated at high thrust values.

3. The key to good performance is a blade that is elliptically loaded. A wake survey of the RB-CCR model in hover would establish the spanwise loading on the blades and thus provide insight into the rotor inflow during hover.

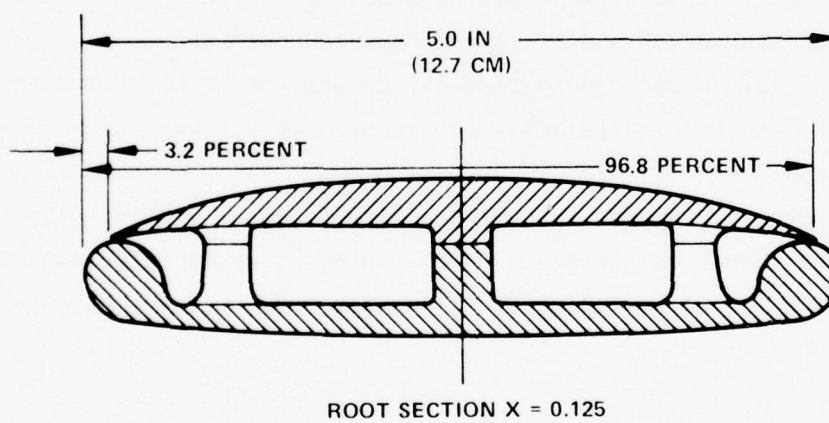
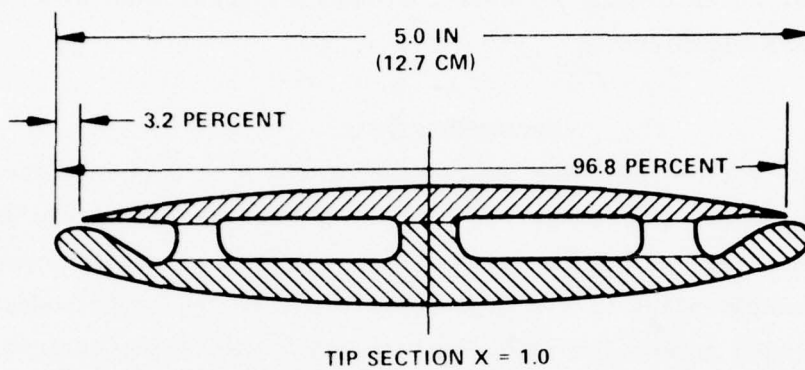


Figure 1 - RB-CCR Model Rotor Tip and Root Airfoil Profiles

Figure 2 - RB-CCR Model on DTNSRDC Hover Stand

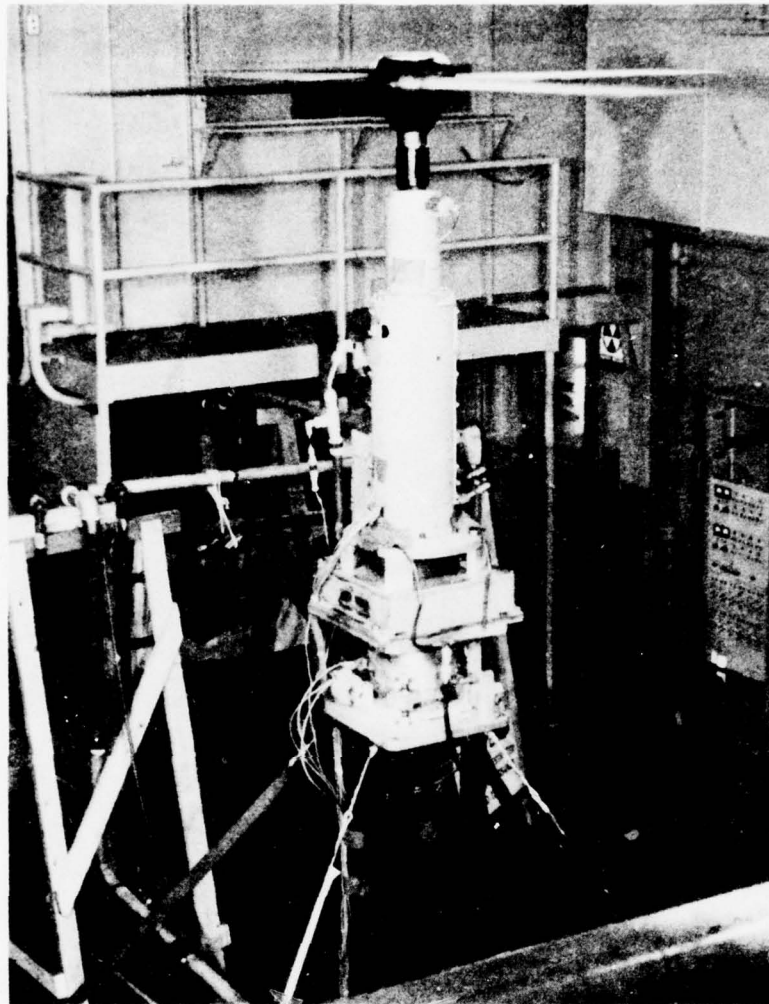


Figure 2a - Experimental Arrangement

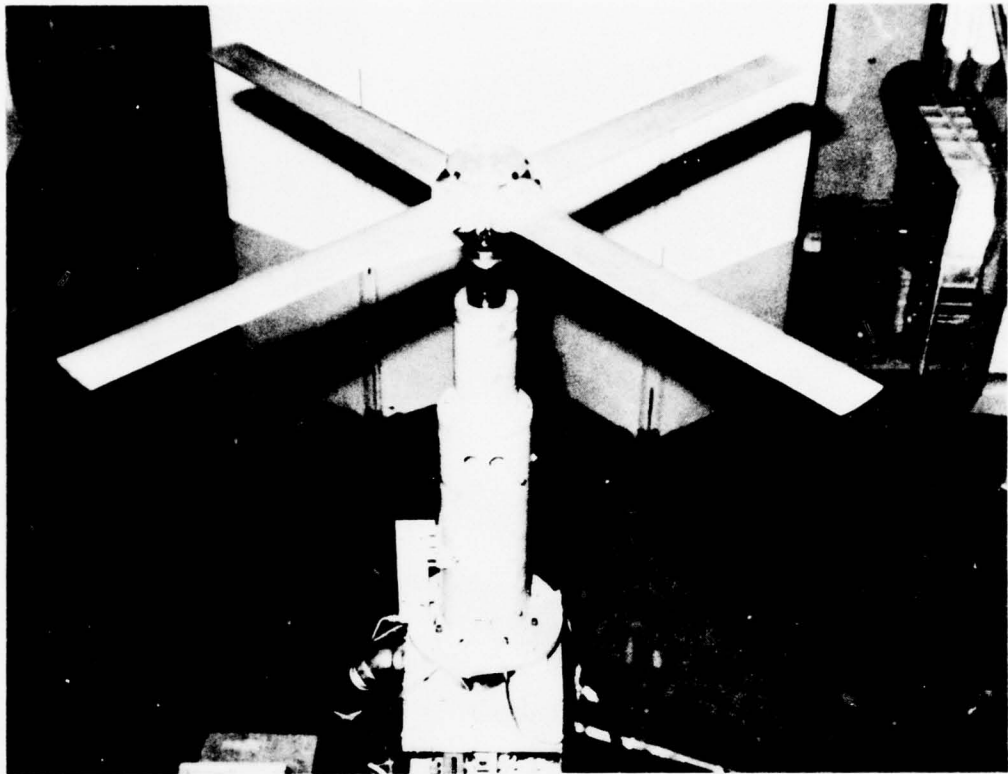


Figure 2b - Closeup View of Model

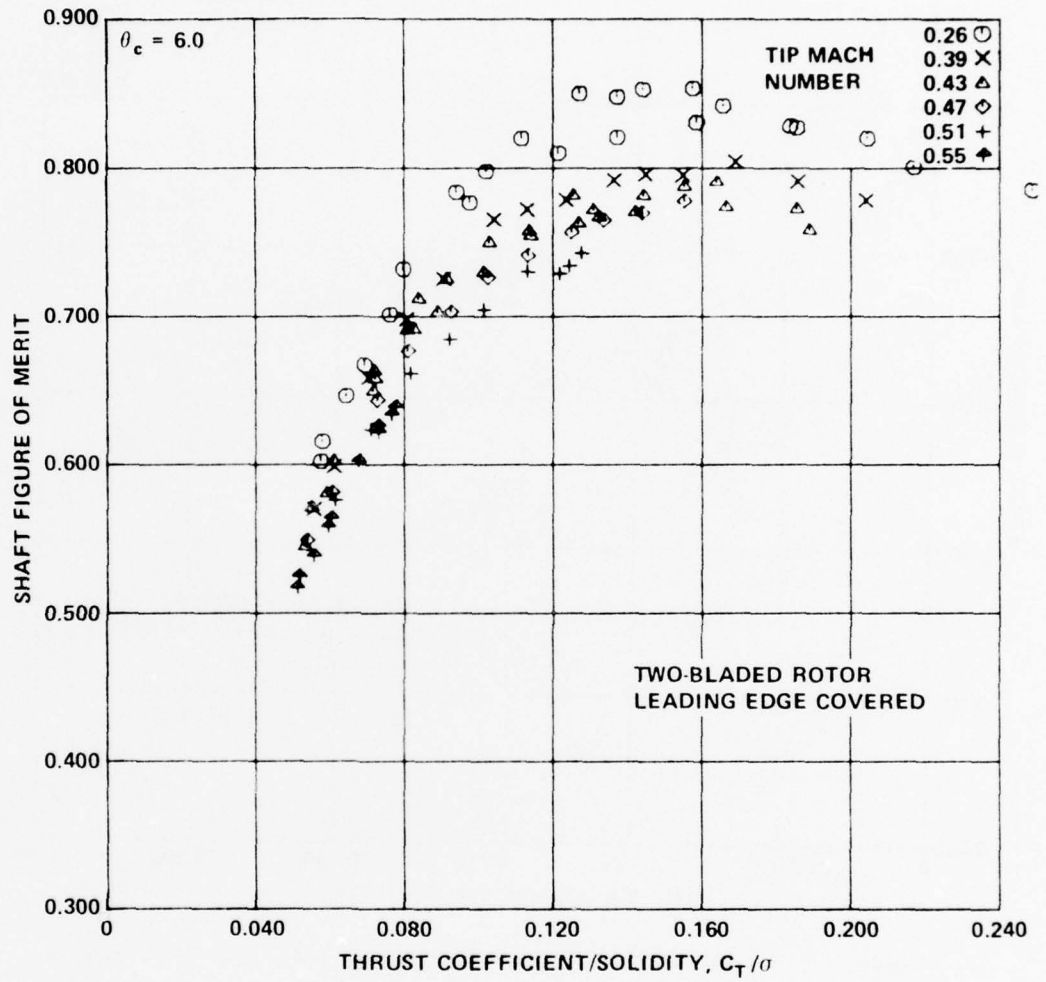


Figure 3 - Effect of Tip Mach Number on Shaft Figure of Merit

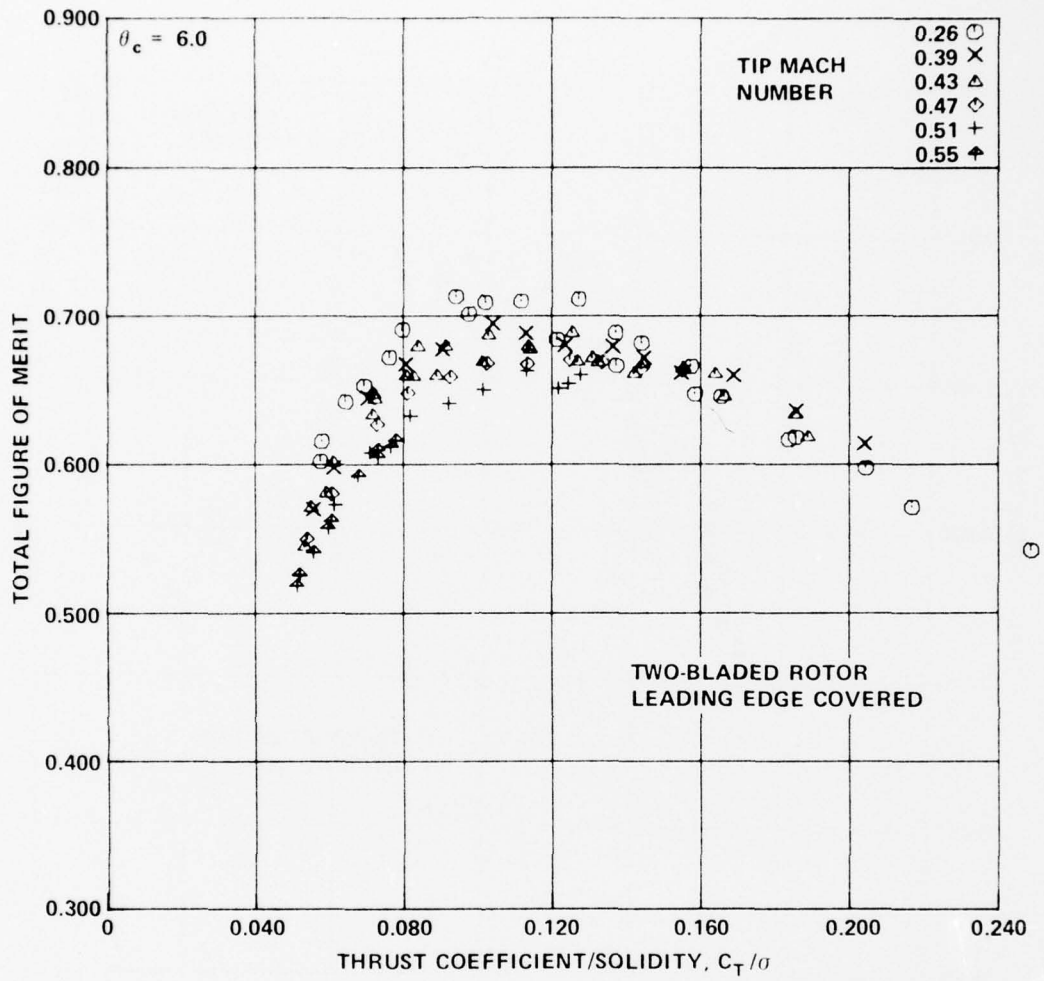


Figure 4 - Effect of Tip Mach Number on Total Figure of Merit

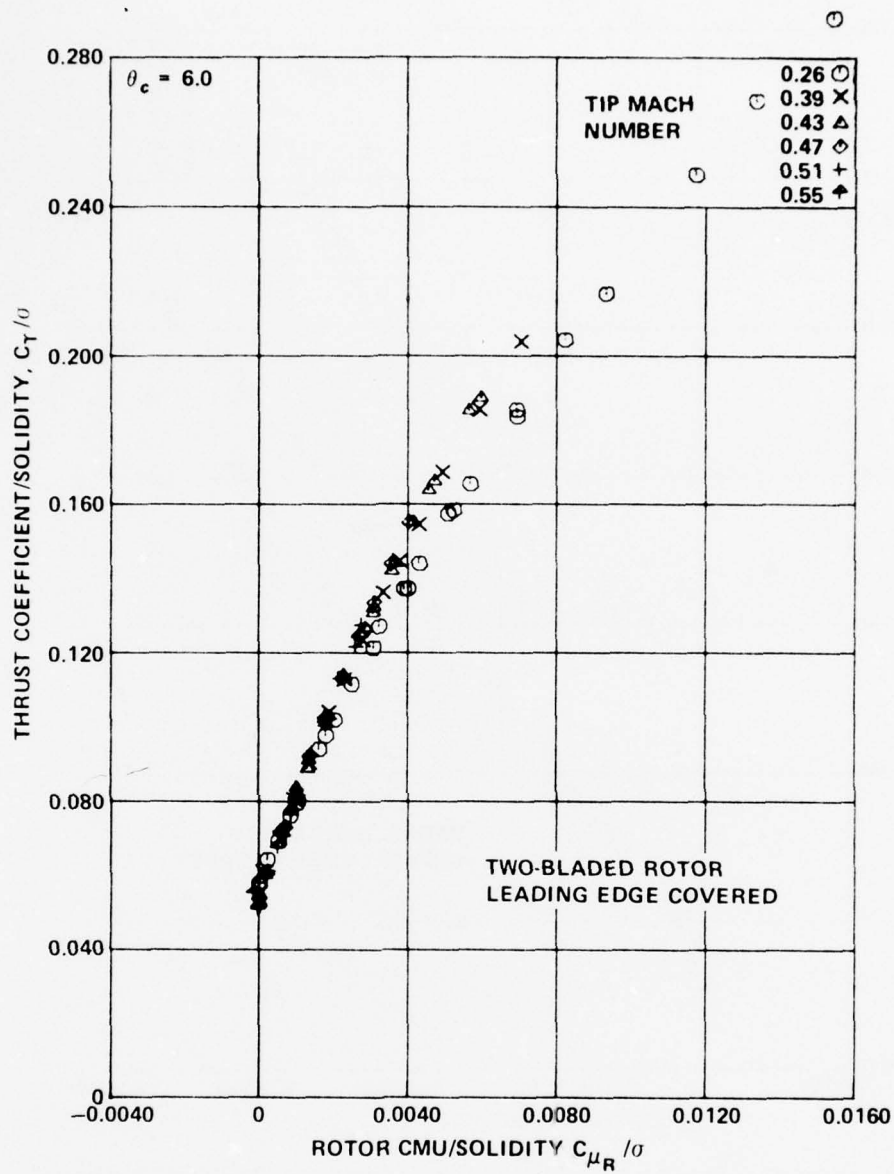


Figure 5 - Effect of Tip Mach Number on Rotor Thrust Augmentation

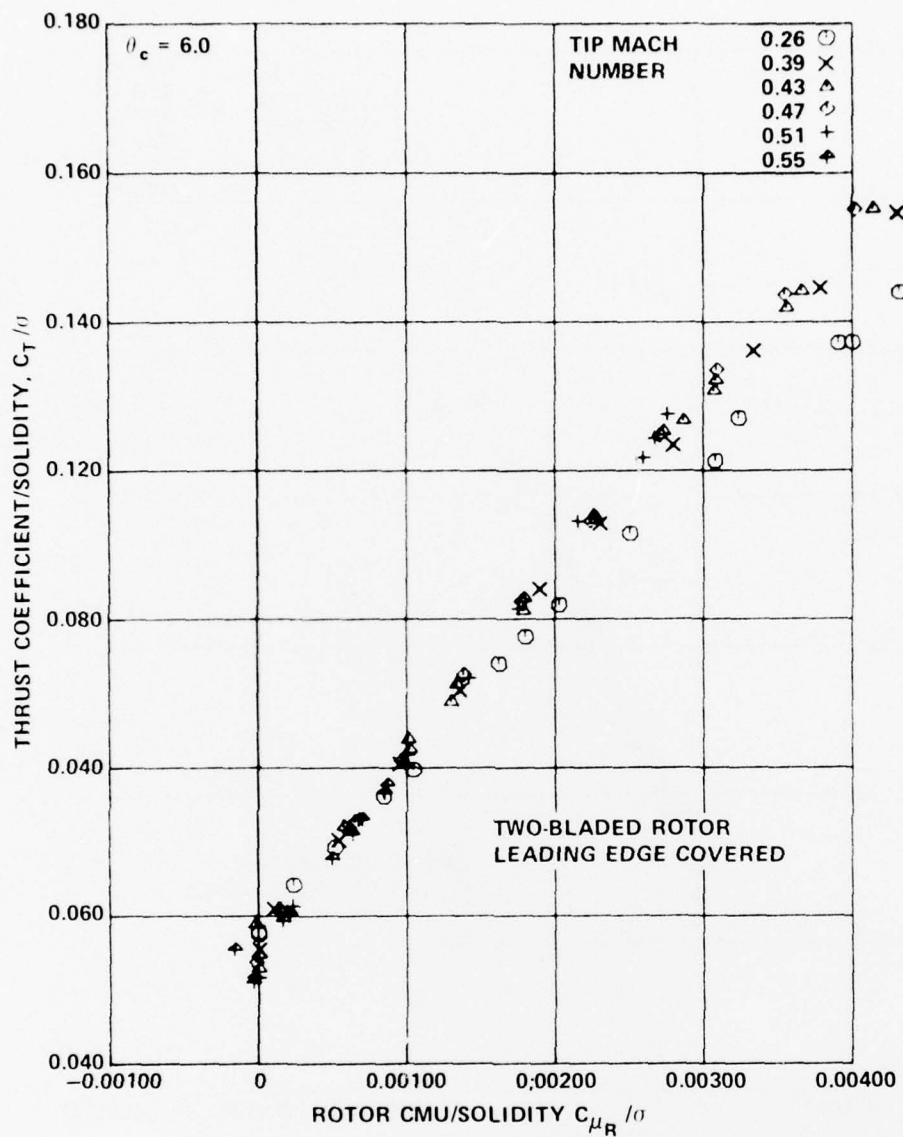


Figure 6 - Expanded Scales to Illustrate Effect of Tip Mach Number on Rotor Thrust Augmentation

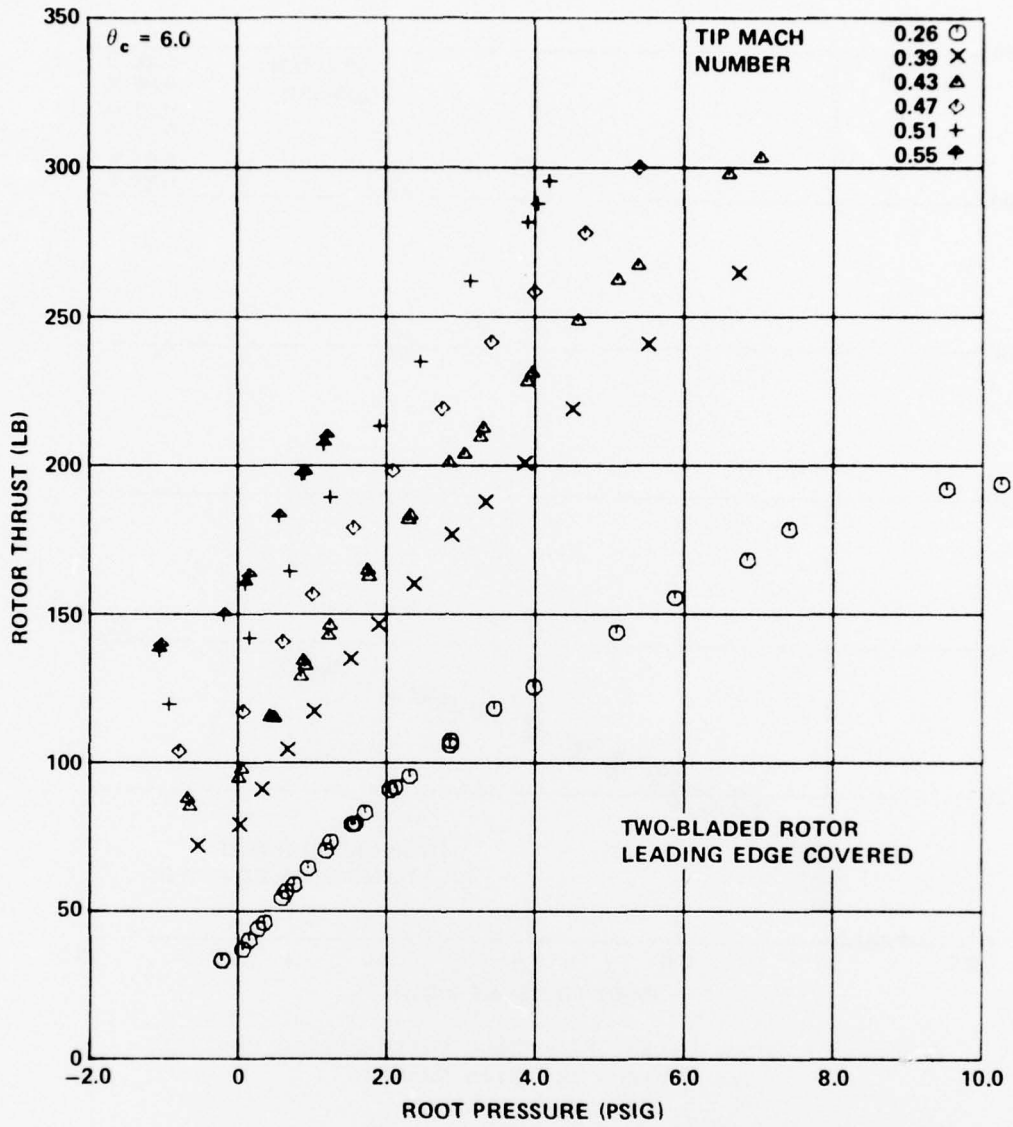


Figure 7 - Rotor Thrust versus Blade Pressure at Various Tip Mach Numbers

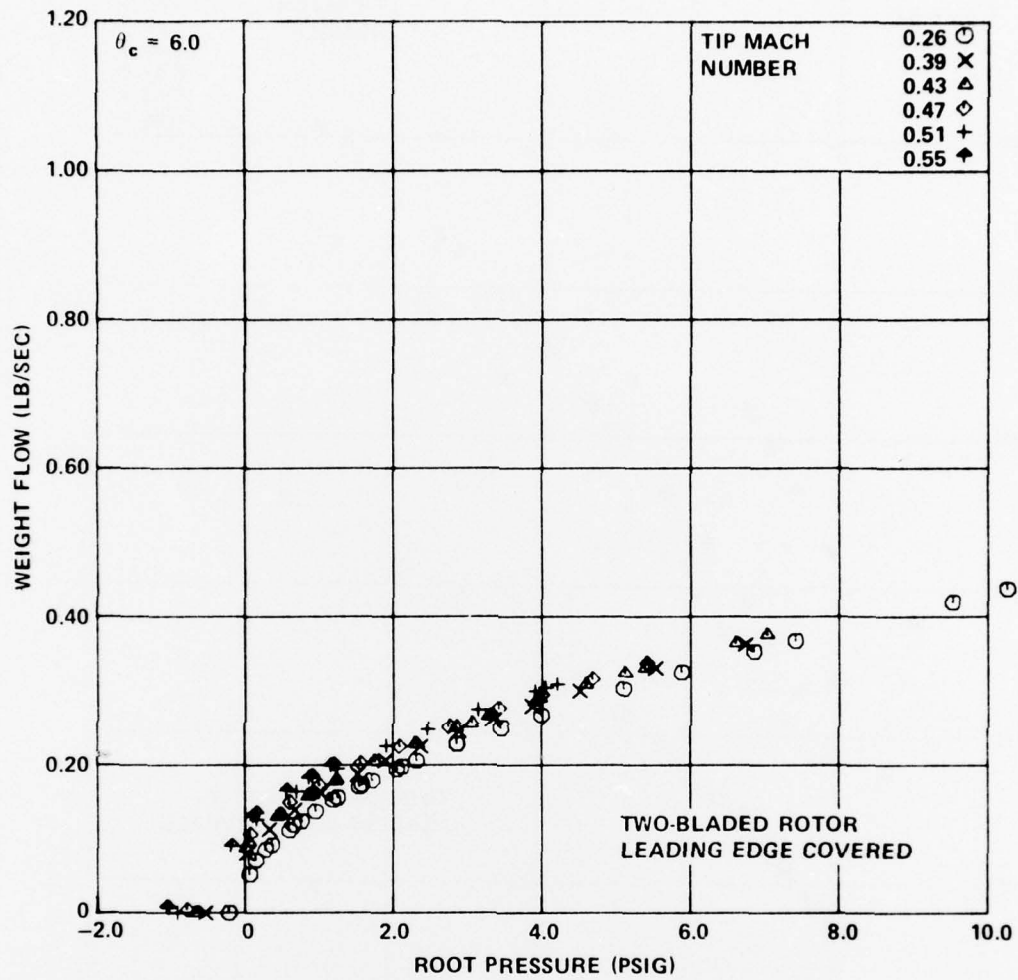


Figure 8 - Rotor Weight Flow Rate versus Blade Pressure at Various Tip Mach Numbers

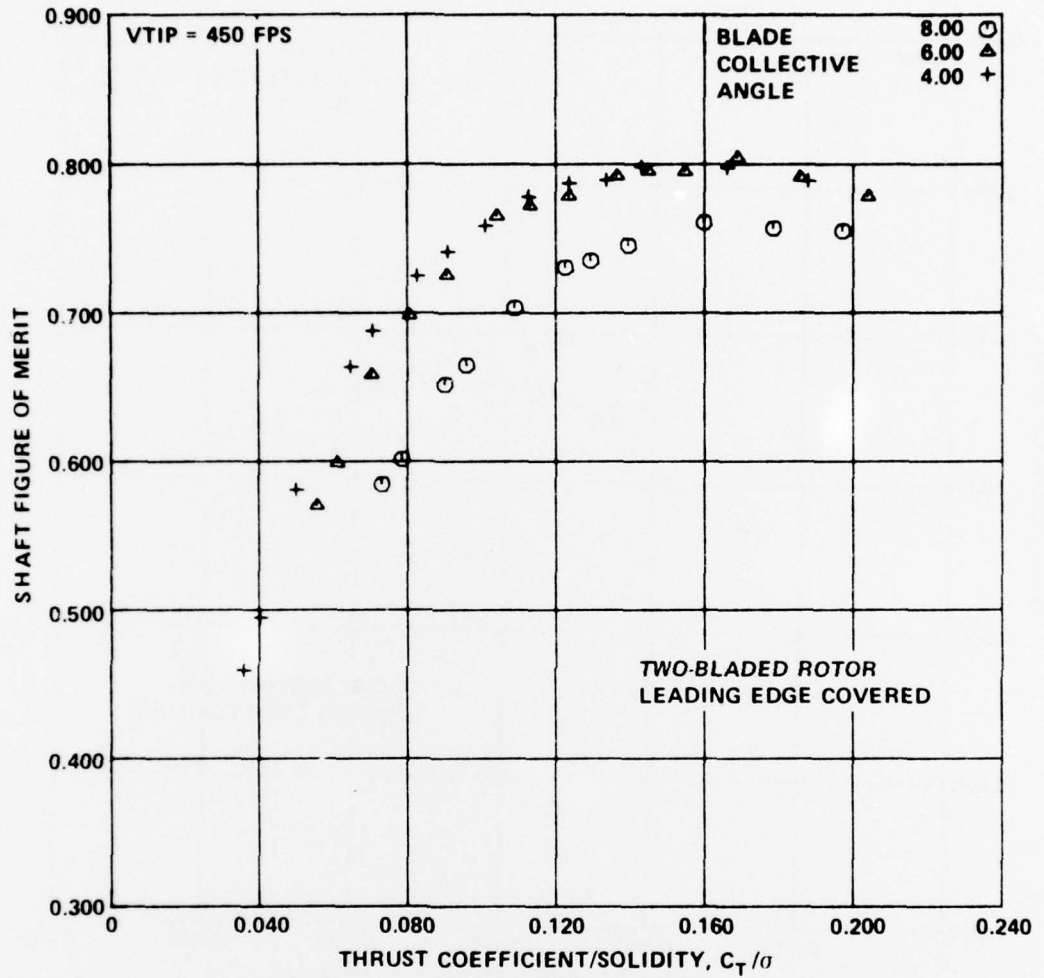


Figure 9 - Effect of Collective Pitch Angle on Shaft Figure of Merit

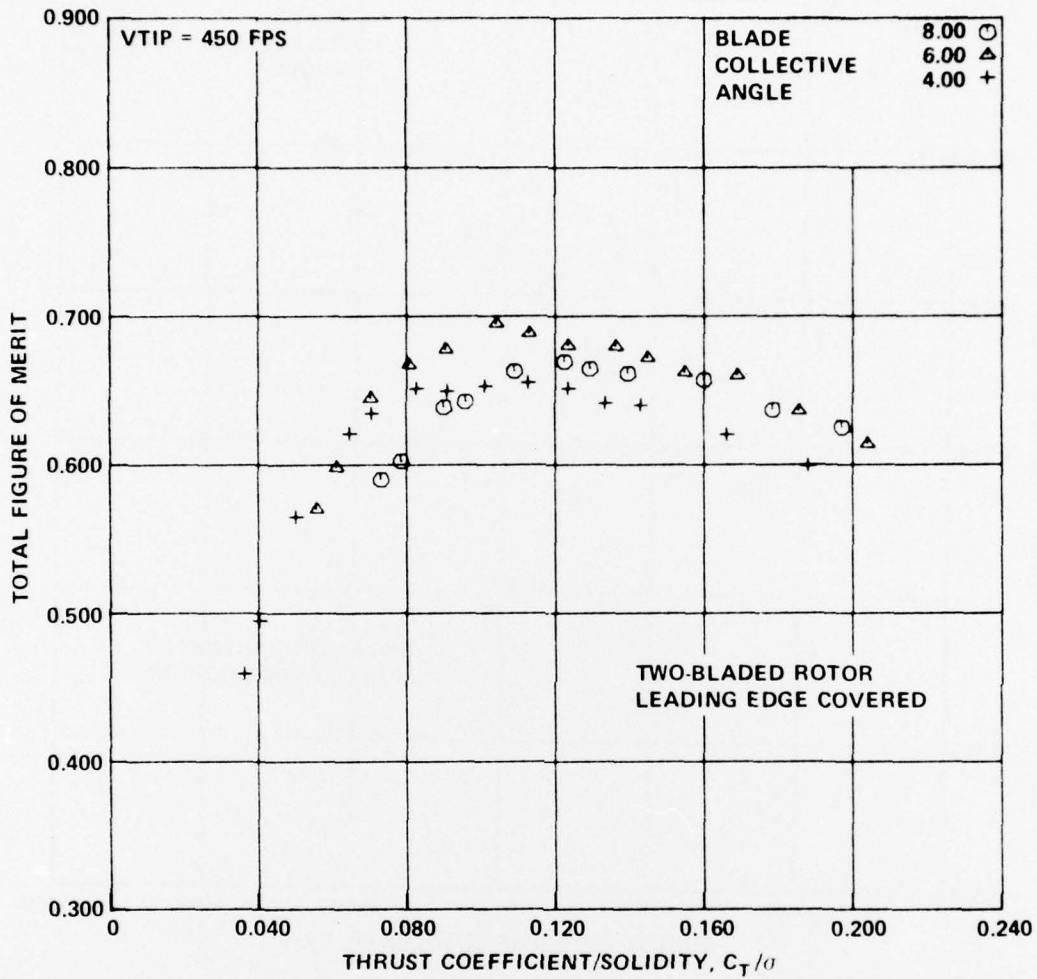


Figure 10 - Effect of Collective Pitch Angle on Total Figure of Merit

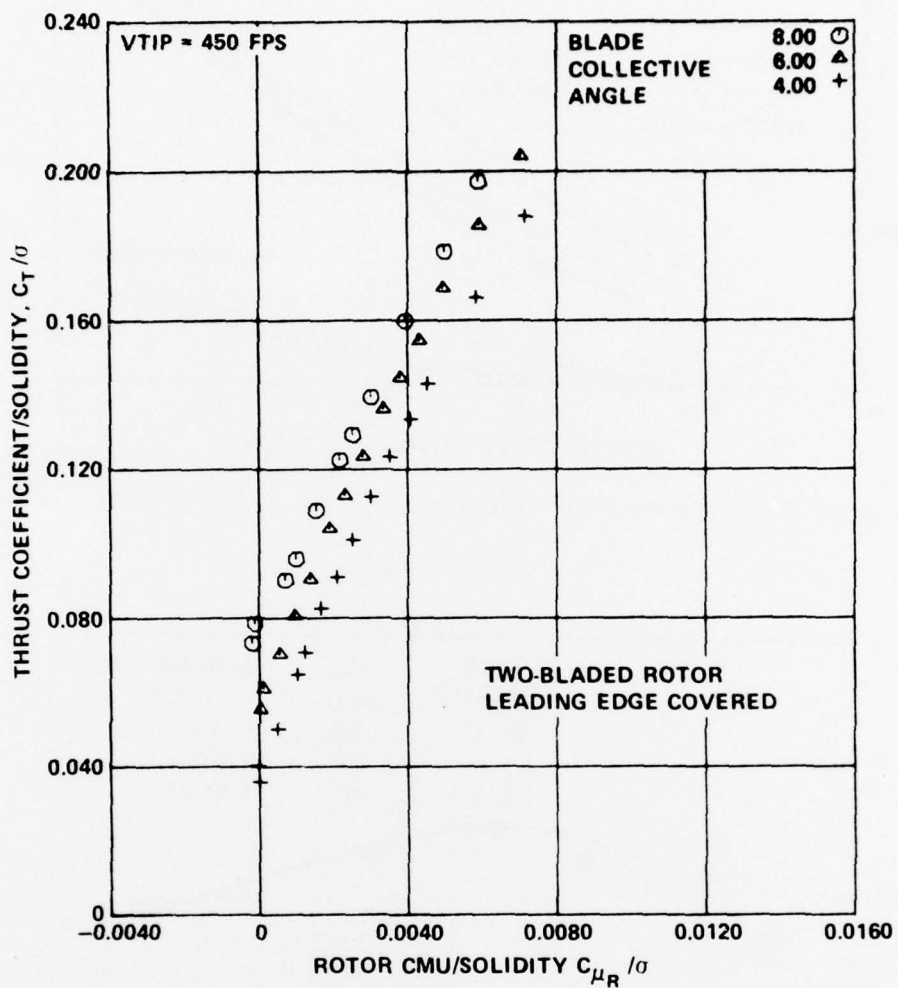


Figure 11 - Effect of Collective Pitch Angle on Rotor Thrust Augmentation

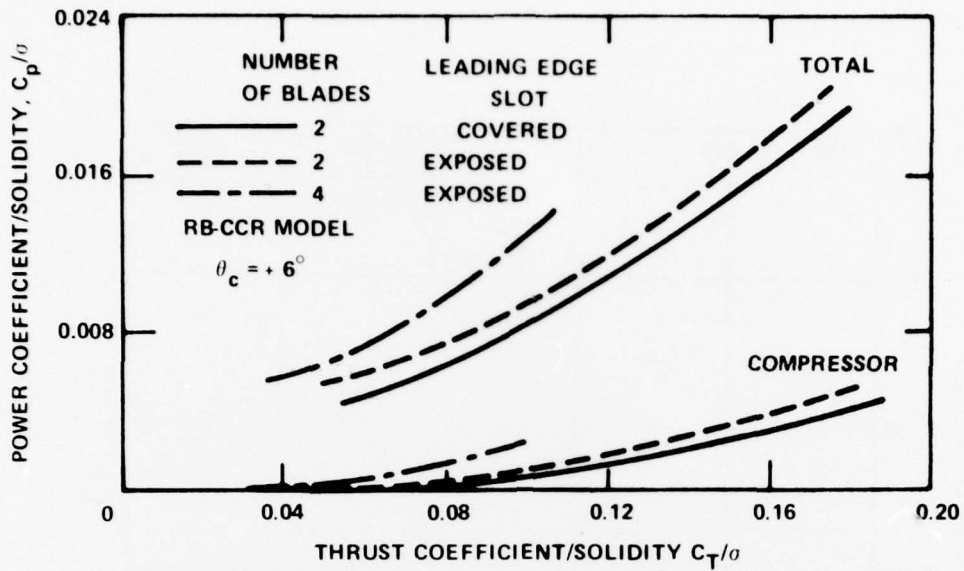


Figure 12 - Leading Edge Slot and Solidity Effects in Hover

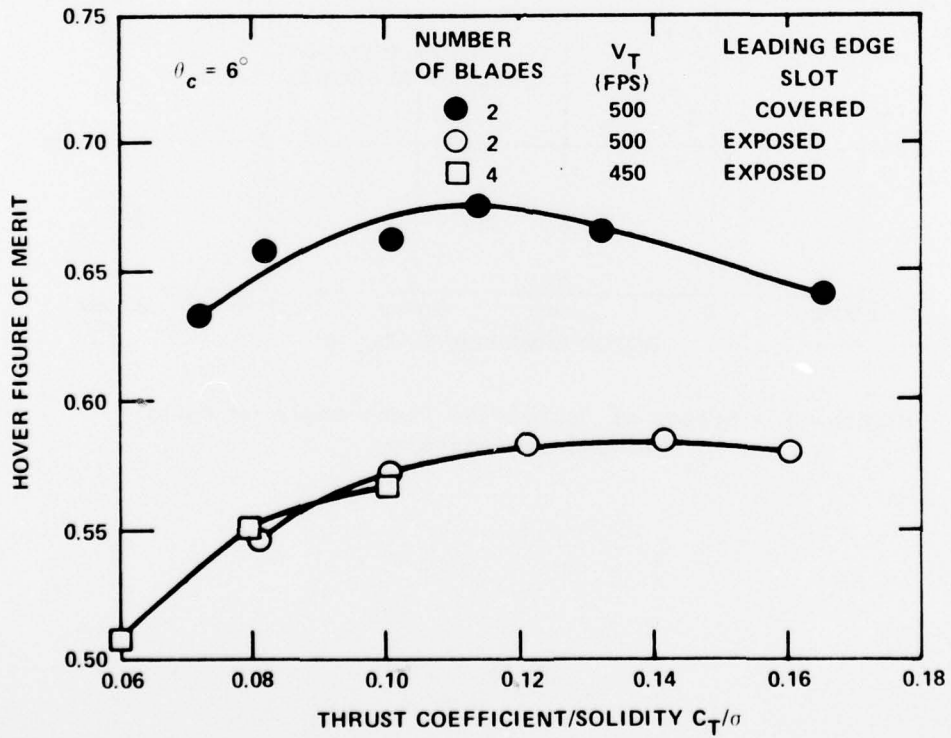


Figure 13 - Hover Performance of Two- and Four-Bladed RB-CCR Rotor

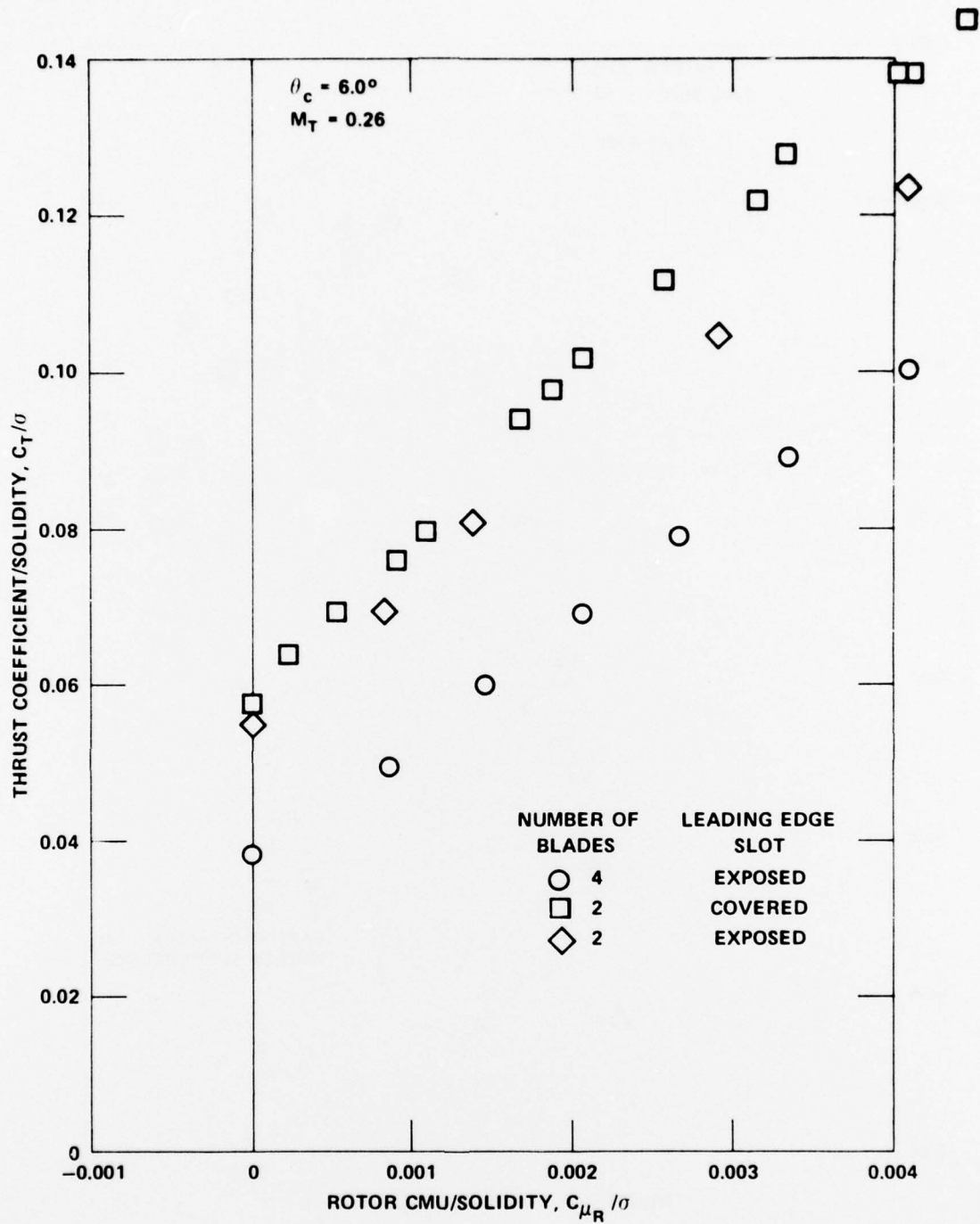


Figure 14 - Effect of Rotor Configuration on Rotor Thrust Augmentation

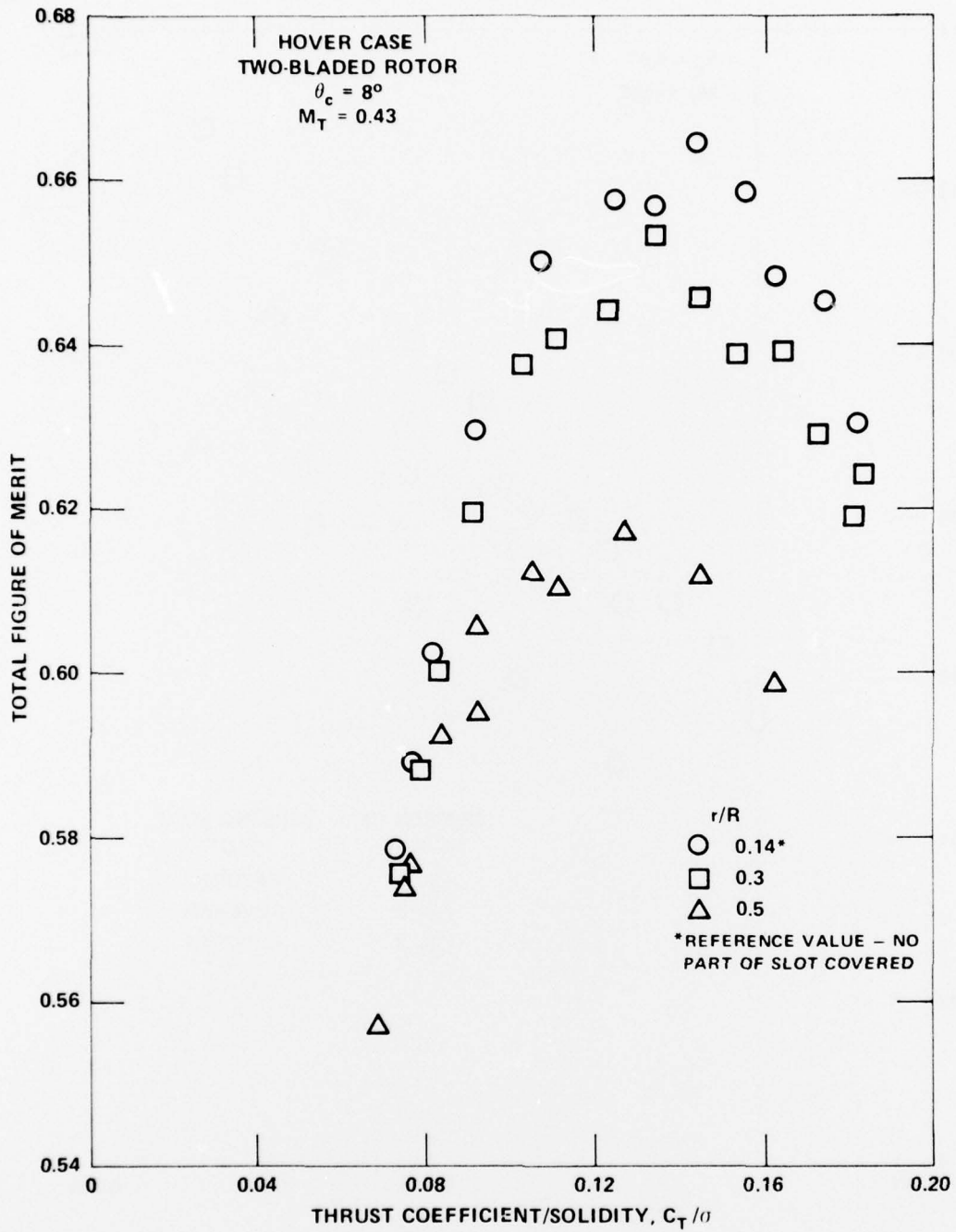


Figure 15 - Effect of Slot Cutout with Leading Edge Covered

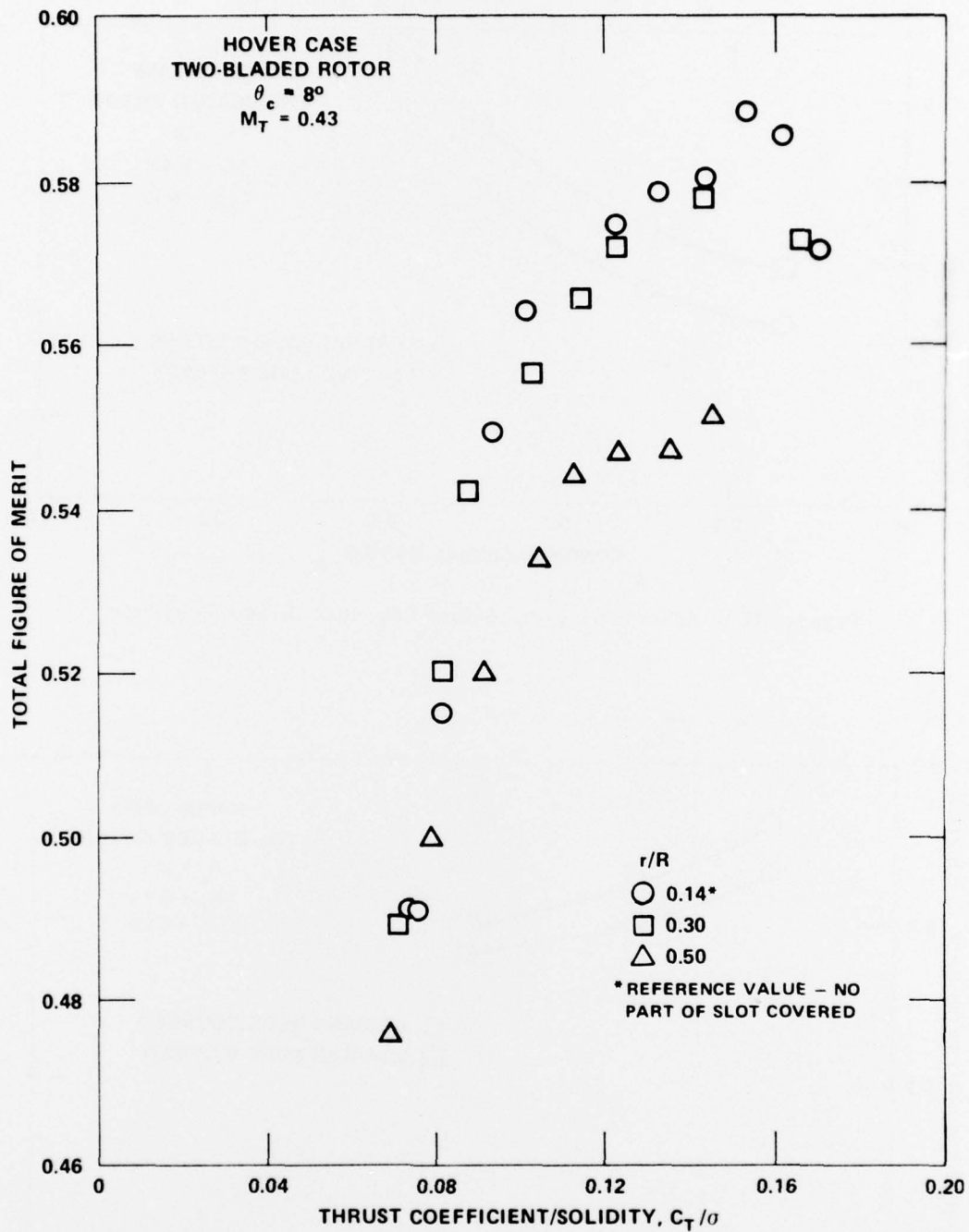


Figure 16 - Effect of Slot Cutout with Leading Edge Exposed

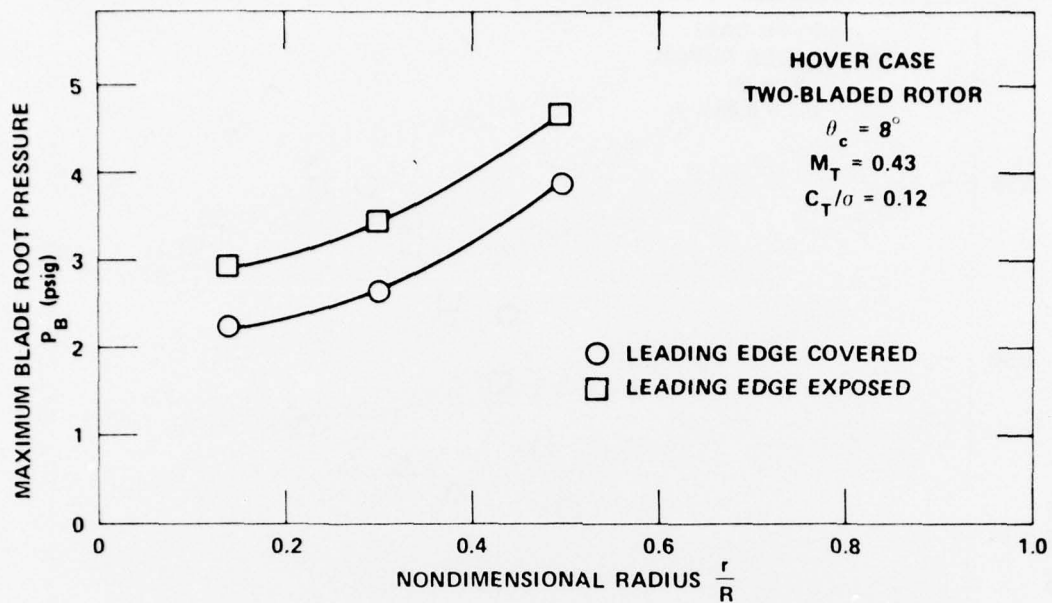


Figure 17 - Effect of Root Cutout on Root Blade Pressure

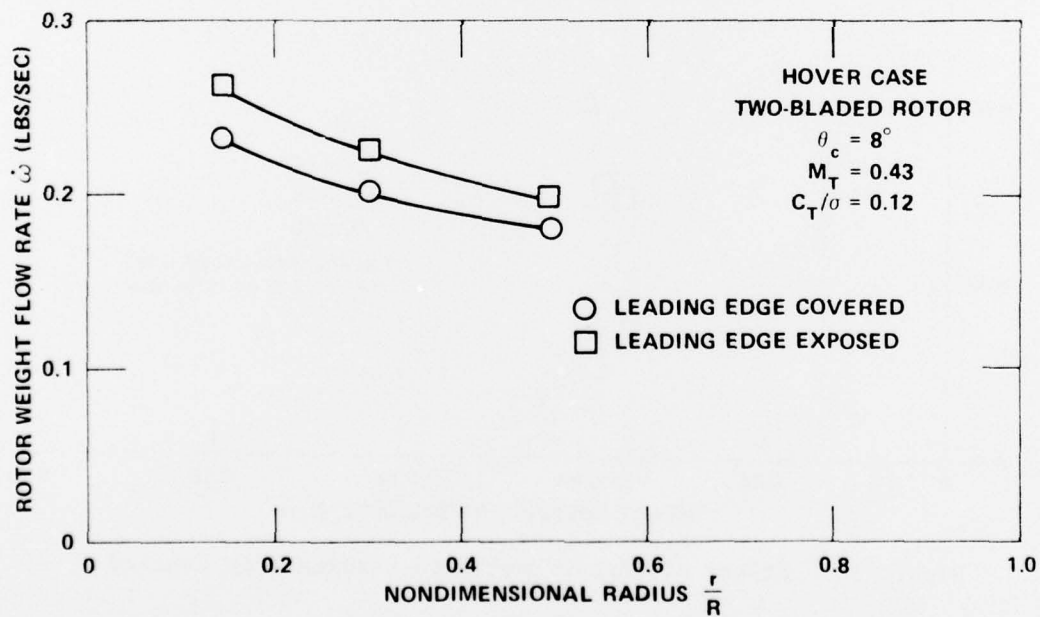


Figure 18 - Effect of Root Cutout on Rotor Weight Flow Rate

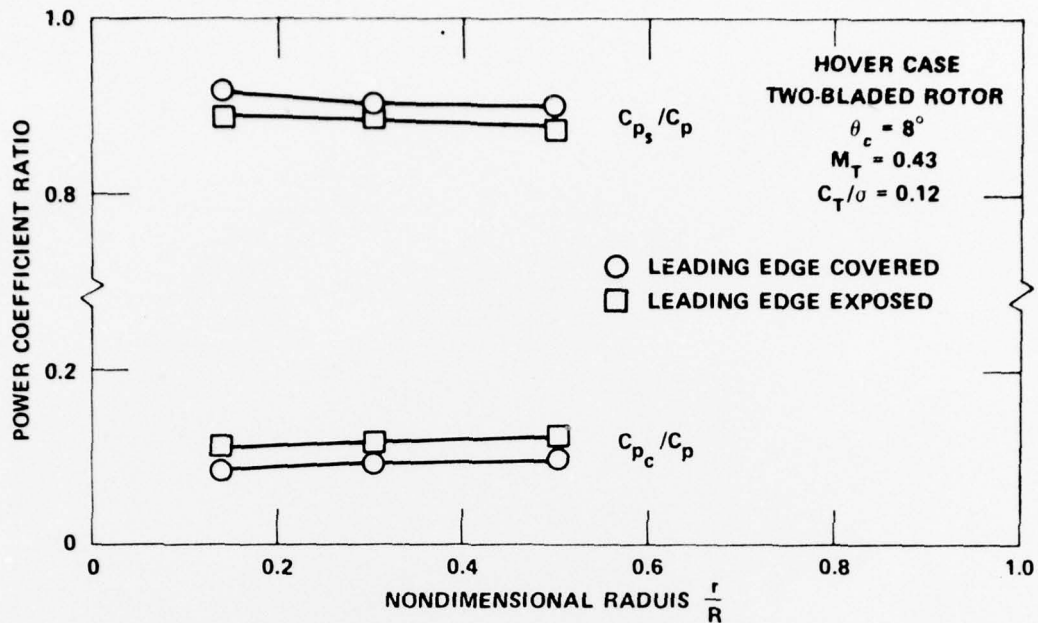


Figure 19 - Effect of Root Cutout on Compressor Power Ratio

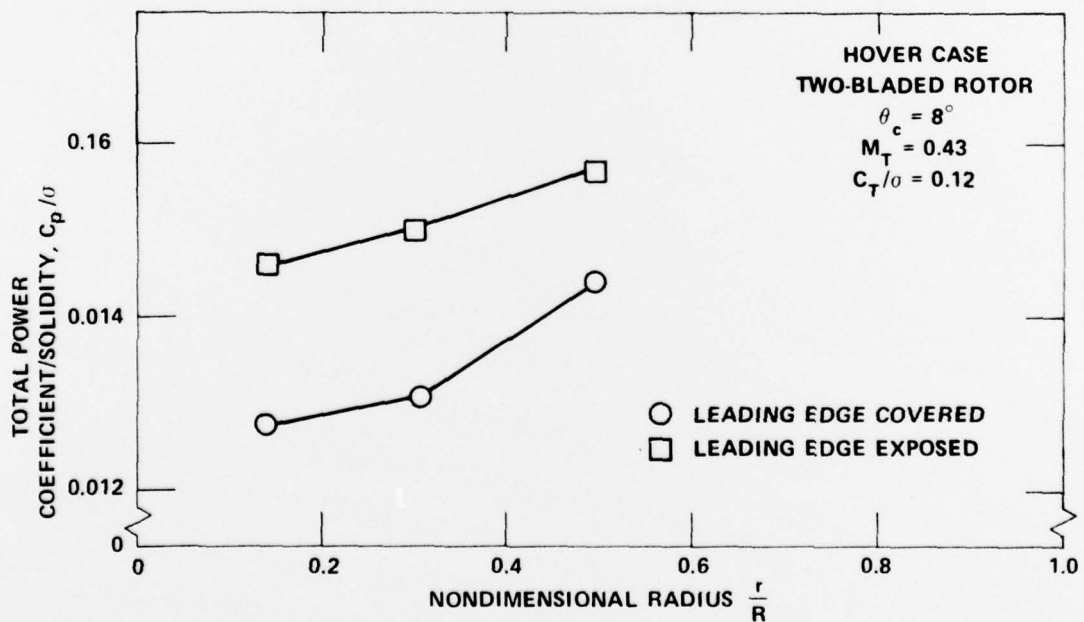


Figure 20 - Effect of Root Cutout on Total Rotor Power

INITIAL DISTRIBUTION

Copies		Copies	
1	MAC/AMCRD-FA	2	NAVAIRTESTCEN
1	ARO/Engr Sci Div		1 Dir TPS
	S. Kumar, Assoc Dir		1 N. Jubeck
1	AASC/Lib	12	DDC
1	AAMCA/AMXAM-SM	1	AF Dep Chief of Staff
2	AAMRD/Lt. Eustis		AFRDT-EX
	1 Lib	2	AFFDL
	1 SAVRE-AM		1 FDV, VTOL Tech Div
2	AAMRD/Ames Res Cen		1 FDMM, Aeromech Br
	1 Tech Dir	1	AFOSR/Mechanics Div
	1 A. Kerr	1	FAA, Code, DS-22
1	CMC/Sci Advisor		V/STOL Programs
	A.L. Slafkosky	3	NASA HQ
1	CHONR/Aeronautics, Code 461		1 A. Evans
2	NRL		1 A. Gessow
	1 Tech Info Office		1 J. Ward (MS-85)
	1 Lib, Code 2029	6	NASA Ames Res Cen
1	USNA		1 Tech Lib
2	NAVPSCOL		1 Full-Scale Res Div
	1 J. Miller		1 M. Kelley/Lg-Scale
	1 L. Schmidt		Aero Br
4	NAVAIRDEVCEEN		1 R.T. Jones
	1 Tech Dir		1 J. McCloud
	1 Tech Lib		1 J. Rabbot
	1 R. McGiboney	4	NASA Langley Res Cen
	1 G. Woods		1 Tech Lib
16	NAVAIRSYSCOM		1 R. Houston
	1 AIR 03		1 L. Jenkins
	1 AIR 03A (F. Tanczos)		1 R. Tapscott
	1 AIR 03PA (W. Koven)	1	Va Inst Tech/Dept Engr
	1 AIR 03P (Capt R.J. Miller)		Mech/D.T. Mook
	2 AIR 320D (R. Siewert)	2	West Va U/Dept Aero Engr
	4 AIR 320B (A. Somoroff)		1 J. Fannuci
	1 AIR 5104		1 J. Loth
	1 AIR 530A (H. Andrews)	1	Analytical Methods/
	1 AIR 5301 (F. Paglianete)		F. Drorak
	1 AIR 530214A (R. Malatino)	1	Bell Aerospace Corp/Ft.
	1 AIR 530112 (R. Tracey)		Worth/Lib
	1 AIR PMA-247		
	(CDR Friichtenicht)		

Copies

2 Boeing Co/Seattle  
 1 Tech Lib  
 1 P.E. Ruppert

2 Boeing Co/Vertol Div  
 1 Tech Lib  
 1 W.Z. Stepniewski

1 Fairchild-Hiller/Farmingdale  
 1 Republic Aviation Div

1 Gen Dyn/Convair Div  
 Tech Lib

1 Grumman Aerospace Corp  
 M. Siegel

2 Honeywell, Inc/S&R Div  
 1 Tech Lib  
 1 R. Rose

2 Hughes Tool Co/Culver City  
 1 E. Wood  
 1 A/C Div

3 Kaman Aerospace Corp  
 1 Tech Lib  
 1 D. Barnes  
 1 A. Lemnios

1 Ling-Temco-Vought, Inc/Lib

4 Lockheed A/C Corp/Burbank  
 1 Tech Lib  
 1 P. Kesling  
 1 E. Martin  
 1 B.R. Rich

1 Lockheed-Georgia Corp/Lib

1 McDonnell-Douglas/Long Be  
 T. Cebeci

1 Northrop Corp/Hawthorne  
 Lib

1 Paragon Pacific Inc.  
 J.H. Hoffman

1 Piasecki Aircraft Corp

1 Rochester Appl Sci Assoc,  
 Inc/Lib

Copies

2 Teledyne Ryan  
 Aeronautical  
 1 P.F. Girard  
 1 Lib

1 United A/C Corp/E.  
 Hartford

3 United A/C Corp/  
 Sikorsky  
 1 Lib  
 1 T. Carter  
 1 I. Fradenburgh

1 Vizex, Inc/R.A.  
 Piziali

CENTER DISTRIBUTION

Copies	Code	
30	5214.1	Reports Distribution
1	5221	Library (C)
1	5222	Library (A)
2	5223	Aerodynamics Lib

**DTNSRDC ISSUES THREE TYPES OF REPORTS**

**(1) DTNSRDC REPORTS, A FORMAL SERIES PUBLISHING INFORMATION OF PERMANENT TECHNICAL VALUE, DESIGNATED BY A SERIAL REPORT NUMBER.**

**(2) DEPARTMENTAL REPORTS, A SEMIFORMAL SERIES, RECORDING INFORMATION OF A PRELIMINARY OR TEMPORARY NATURE, OR OF LIMITED INTEREST OR SIGNIFICANCE, CARRYING A DEPARTMENTAL ALPHANUMERIC IDENTIFICATION.**

**(3) TECHNICAL MEMORANDA, AN INFORMAL SERIES, USUALLY INTERNAL WORKING PAPERS OR DIRECT REPORTS TO SPONSORS, NUMBERED AS TM SERIES REPORTS; NOT FOR GENERAL DISTRIBUTION.**